

Photoluminescence from $\text{ZnS}_{1-x}\text{Te}_x$ alloys under hydrostatic pressure

Z. L. Fang, G. H. Li, N. Z. Liu, Z. M. Zhu, H. X. Han, and K. Ding

National Laboratory for Superlattices and Microstructures, Institute of Semiconductors, Chinese Academy of Sciences, P.O. Box 912, Beijing 100083, China

W. K. Ge and I. K. Sou

Department of Physics, Hong Kong University of Science and Technology, Clear Water Bay, Kowloon, Hong Kong, China

(Received 26 December 2001; published 6 August 2002)

$\text{ZnS}_{1-x}\text{Te}_x$ ($0.02 \leq x \leq 0.3$) alloys are studied by photoluminescence under hydrostatic pressure at room temperature. Only a wide emission band is observed for each sample. Its peak energy is much lower than the corresponding band gap of alloys. These bands are ascribed to the radiative annihilation of excitons bound at Te_n ($n \geq 2$) isoelectronic centers. The pressure coefficients of the emission bands are smaller than those of alloy band gaps from 48% to 7%. The difference of the pressure coefficient of the emission band and the band gap increases when the binding energy of Te_n centers decreases. It seems contrary to our expectation and needs further analysis. The integrated intensities of emission bands decrease with increasing pressure due to the decreasing of the absorption coefficient associated with the Te_n centers under pressure. According to this model the Stokes shifts between the emission and absorption bands of the Te_n centers are calculated, which decrease with the increasing Te composition in alloys.

DOI: 10.1103/PhysRevB.66.085203

PACS number(s): 71.55.Gs, 62.50.+p, 78.55.Et

I. INTRODUCTION

In recent years, semiconductor alloys with a large bowing factor have been attracting much attention because of their distinct properties from normal semiconductor alloys. It was shown in recent research about GaNAs and InGaNAs that the interaction between N isoelectronic traps and the conduction band edge of GaAs and InGaNAs has a great effect on their band structures.^{1,2} A similar effect has also been observed in the Te-rich ZnSTe alloys.^{3,4} On the other hand, As and Te atoms can form isoelectronic centers in N-rich GaNAs and S-rich ZnSTe alloys, respectively.⁵⁻¹⁰ A hole is bound at these centers by a short-range potential resulting from the large difference of electronegativities between S and Te or N and As atoms. An electron is then bound Coulombically to form a bound exciton. Thus the properties of these isoelectronic centers are mainly related to the valence bands of host materials. An investigation of the Te and As isoelectronic centers in ZnSTe or GaNAs alloys may give more information about the band structure of alloys with a large bowing factor and the interaction between isoelectronic center and host band.

Due to the difficulty in sample growth, there are few works on As isoelectronic centers in N-rich GaNAs alloys. And the early works about Te centers in S-rich ZnSTe alloys are limited in the range of Te composition less than 0.1.⁷⁻¹⁰ Recent advances of molecular-beam epitaxy (MBE) technology made the growth of ZnSTe alloys with whole composition possible.^{4,5} It then gives the possibility of investigation of the Te isoelectronic centers in the ZnSTe alloys with larger Te composition.

Photoluminescence (PL) under hydrostatic pressure is a powerful tool in the investigation of isoelectronic centers and the band structure of alloys with a large bowing factor. Great success was achieved in the study of GaAs:N and ZnTe:S

alloys.^{1,4} However, these isoelectronic centers are mainly related to conduction bands. There are few reports about the pressure behavior of Te isoelectronic centers in ZnS or ZnSTe alloys.

In this paper, we investigate the PL under hydrostatic pressure of $\text{ZnS}_{1-x}\text{Te}_x$ ($0.02 \leq x \leq 0.3$) alloys. We found that the PL spectra come from deep energy levels in the band gap until $x = 0.3$. They have smaller pressure coefficients than the corresponding band gap and have large Stokes shifts. According to the early work on ZnS:Te (Refs. 7-10) and the pressure behavior of these centers, we attribute the observed emission to the radiative recombination of excitons bound to Te_n ($n \geq 2$) isoelectronic centers. In order to have an overall understanding about the dependence of the properties of these centers on Te composition, some results published earlier⁶ are also included in this paper.

II. SAMPLES AND EXPERIMENTS

The $\text{ZnS}_{1-x}\text{Te}_x$ alloy samples used in this study were grown on (001) GaAs substrates by using the VG V80H MBE system. The thicknesses of the epilayers are listed in Table I. The Te composition was determined by using energy-dispersive x-ray spectrometry. They are 0.02, 0.08, 0.15, 0.21, 0.25, and 0.30 for samples A, B, C, D, E, and F, respectively. Details of sample growth have been described elsewhere.⁵ For PL measurements under high pressure, the samples were back thinned to about 20 μm thick by mechanical polishing and then cut into pieces of about $100 \times 100 \mu\text{m}^2$ in size. The hydrostatic pressure was generated by a diamond anvil cell. The 4:1 methanol-ethanol mixture was used as pressure-transmitting medium. The pressure was monitored by the spectral shift of the R_1 line of ruby. The PL spectra under hydrostatic pressure were measured at room temperature by using 406.7, 488.0, and 325.0 nm lines of

TABLE I. Sample parameters, binding energy E_b , relative binding energy ε_b , pressure coefficient of PL spectra α , and Stokes shift E_S for $\text{ZnS}_{1-x}\text{Te}_x$.

	x	Thickness $d(\mu\text{m})$	E_b (eV)	ε_b	α (meV/GPa)	E_S (eV)
A	0.02	1.8	0.87	0.24	53(3)	0.92(4)
B	0.08	2.8	0.88	0.27	62(3)	0.41(5)
C	0.15	2.3	0.68	0.23	50(3)	0.46(5)
D	0.21	1.6	0.58	0.21	45(2)	0.10(4)
E	0.25	0.8	0.49	0.18	39(2)	0.14(6)
F	0.30	0.36	0.38	0.15	39(2)	0.18(5)

Kr^+ , Ar^+ , and He-Cd lasers as the source of excitation. The emitted light is dispersed by a JY-HRD2 double-grating monochromator and detected by a GaAs photomultiplier.

III. RESULTS AND DISCUSSIONS

A. PL spectra at normal pressure

In Fig. 1 the normalized room-temperature PL spectra under ambient pressure of the six samples are shown in the sequence of Te composition x . Samples D, E, and F were excited by the 488.0 nm line of an Ar^+ laser, B and C by the 406.7 nm line of a Kr^+ laser, and A by the 325.0 nm line of a He-Cd laser, respectively. Most of the samples have multipeak structures and show regular periodic oscillations apparently. These multipeak structures have been proved to be optical interference.¹¹ The reflection spectrum of sample B is

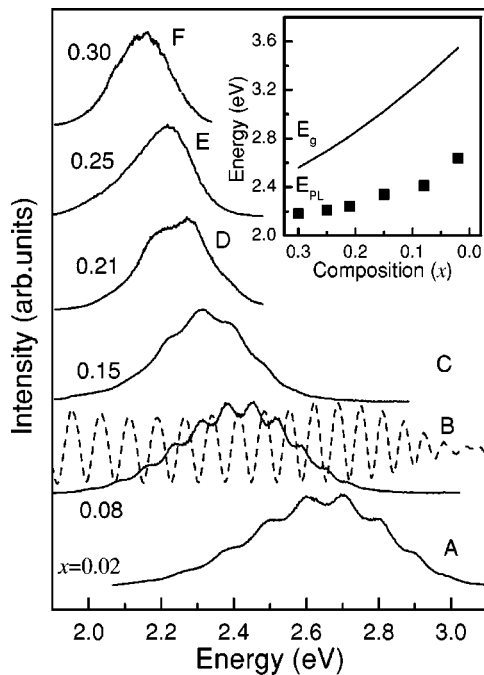


FIG. 1. Normalized PL spectra (solid lines) of six $\text{ZnS}_{1-x}\text{Te}_x$ alloys under ambient pressure at 300 K. Dashed line is the reflection spectrum of sample B. The variations of PL peak energy (solid squares) and corresponding band gap (solid line) are shown in the inset as a function of Te composition.

also drawn in Fig. 1 by the dashed line to confirm the interference effect. The PL peaks of $\text{ZnS}_{1-x}\text{Te}_x$ alloys with $x = 0.01-0.03$ have been well assigned as the radiative recombination of excitons bound to Te_2 isoelectronic centers.⁷⁻¹⁰ Goede *et al.*⁹ have reported that the PL peak energy of $\text{ZnS}_{1-x}\text{Te}_x$ film with $x = 0.02$ is about 2.65 eV at 300 K under ambient pressure. The measured PL peak energy of our sample A ($x = 0.02$) is 2.68 eV. Thus we attribute the emission of sample A to the Te_2 centers too. In fact, PL emission from Te_n centers has been observed in many telluride II-VI ternary alloys with larger Te composition values. Reznitsky *et al.*¹² reported the PL spectra of $\text{ZnSe}_{1-x}\text{Te}_x$ alloys with Te composition up to 0.22. In the work of Goede *et al.* about $\text{CdS}_{1-x}\text{Te}_x$ alloys the Te composition is up to 0.2.¹³ In all these work, the PL peaks have been assigned as Te isoelectronic centers or Te_n clusters. Since our samples are unintentionally doped, we also attribute the PL peaks of our samples to the emissions from Te_n centers in the ZnSTe alloy; even the highest Te composition value is 0.3 in our case.

The Te composition dependences of the PL peak energy E_{PL} (solid squares) and corresponding band gap of alloys, E_g (solid line), are drawn together in the inset of Fig. 1. The band gap of the $\text{ZnS}_{1-x}\text{Te}_x$ alloy is obtained by transmission measurements of the same series of sample.⁵ It can be expressed as

$$E_g(x) = xE_{ZnTe} + (1-x)E_{ZnS} - bx(1-x), \quad (1)$$

where b is the bowing factor and equal to 3.37 eV; E_{ZnTe} and E_{ZnS} denote the band gaps of ZnTe and ZnS, and are equal to 2.40 eV and 3.64 eV, respectively. We define the binding energy of the centers corresponding to the PL spectra as $E_b = E_g - E_{PL}$. Because the band gap varies with the Te composition value x , a relative binding energy $\varepsilon_b = E_b/E_g$ is introduced here. All values of E_b and ε_b are listed in Table I. With an increase of x , the values of E_b and ε_b decrease except for sample B ($x = 0.08$). For $\text{ZnS}_{1-x}\text{Te}_x$ alloys with $x = 0.03-0.1$, the PL spectra at about 2.51 eV were ascribed to Te_3 clusters.⁸⁻¹⁰ If we also attribute the PL peak at 2.41 eV for sample B to Te_3 clusters, it is easy to explain the larger values of E_b or ε_b for sample B since larger Te_n clusters will lead to a deeper localized short-range potential and then result in a larger binding energy. When the Te composition increases further, the binding energy decreases monotonically. Since the potential difference between the same Te_n clusters and the host atoms (average of Te and S atoms in the virtual crystal approximation) will decrease with increasing Te composition,^{14,15} the binding energy will decrease with $x(x \geq 0.08)$, if all the PL spectra in these samples come from Te_3 clusters. There is also another possibility that the emission of samples with higher x may come from larger Te_n clusters. In this case the effect of the larger clusters on the localized potential must be smaller than the effect of alloy composition on the potential difference between clusters and the host atoms.

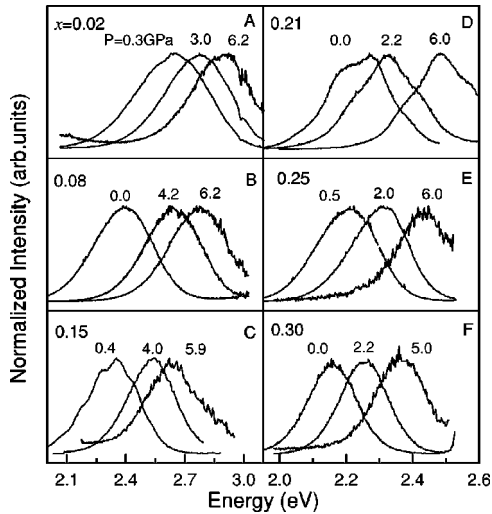


FIG. 2. The normalized room-temperature PL spectra of six $\text{ZnS}_{1-x}\text{Te}_x$ alloys under selected pressures.

B. Dependence of the pressure coefficient on Te composition

Figure 2 is the six sample PL spectra under different pressures. Sample A was excited by the 325.0 nm line, B and C by the 406.7 nm line, and D, E, and F by the 488.0 nm line, respectively. The PL peaks of all the samples exhibit a blueshift with nearly no change in the half-width of the peak bands when the pressure increases. Figure 3 shows the PL peak energy of all the samples as a function of pressure. The solid lines for each sample represent the results of a least-squares fit of experiment data by equation

$$E_{PL}(P) = E_{PL}(0) + \alpha P, \quad (2)$$

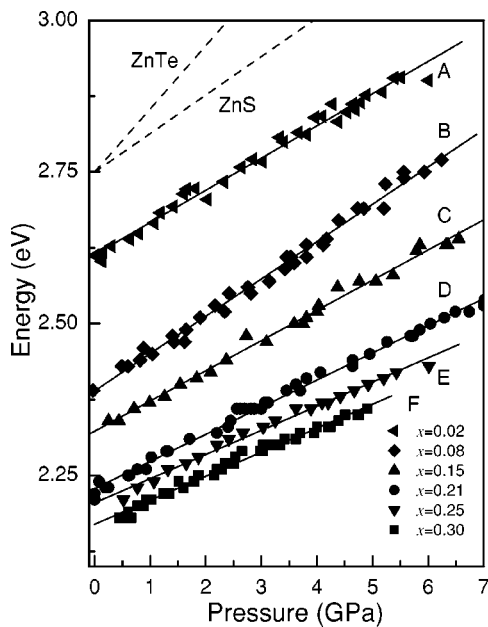


FIG. 3. The pressure dependences of PL peak energies for six $\text{ZnS}_{1-x}\text{Te}_x$ alloys. The solid line is the least-squares fit to the data. The pressure dependences of the band gaps of ZnTe and ZnS (dashed lines) are drawn symbolically too.

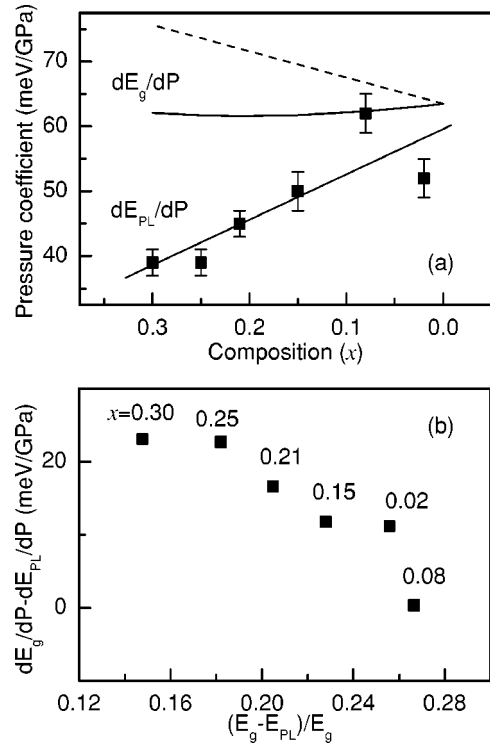


FIG. 4. The Te composition x dependence of the pressure coefficient of the PL peak (a) and the variation of pressure coefficient of the binding energy as a function of the relative binding energy (b). The x dependence of the pressure coefficient of the band gap obtained from linear interpolation (dashed line) and Eq. (3) (upper solid line) is also shown in (a).

where $E_{PL}(0)$ and $E_{PL}(P)$ are the PL peak energy under normal and applied pressure P , respectively, and α the pressure coefficient of the PL peaks. The values of α for different samples are listed in Table I too. The pressure coefficient of ZnTe and ZnS is 104 meV/GPa and 63.5 meV/GPa,¹⁶ respectively. The pressure dependences of the band gap of these two binary compounds are also drawn in Fig. 3 as the upper dashed lines. The lines were vertically shifted for clear comparison. The Te composition dependences of pressure coefficients of six samples are shown in Fig. 4(a). The pressure coefficients decrease with x except for sample B ($x=0.08$). For comparison, we need to know the pressure coefficients of the band gap of alloys. However, there are no experimental results about these coefficients. Normally, the pressure coefficients of the band gap of ternary alloys can be obtained by the linear interpolation of those of binary compounds. The result of the interpolation of $\text{ZnS}_{1-x}\text{Te}_x$ alloys is drawn as a dashed line in Fig. 4(a). In our case, however, the dependence of the bowing factor b on pressure must be included. Then the pressure coefficient of the $\text{ZnS}_{1-x}\text{Te}_x$ band gap can be expressed as

$$\frac{dE_g}{dP} = x \frac{dE_{\text{ZnTe}}}{dP} + (1-x) \frac{dE_{\text{ZnS}}}{dP} - x(1-x) \frac{db}{dP}. \quad (3)$$

According to the Hill-Richardson model,¹⁷ the bowing factor b can be written as

$$b = \frac{\text{const}}{a^4}, \quad (4)$$

where a is lattice constant of ternary alloys. By using Murhan's equation¹⁸

$$-\frac{dP}{d \ln V} = B(P) = B + B'P, \quad (5)$$

where $V \propto a^3$ is the volume and B and B' are the bulk modulus and its pressure derivative, we can express the pressure derivative of b as

$$\frac{db}{dP} = \frac{4b}{3(B+B'P)}. \quad (6)$$

In our calculation, we used the average of B for $x=0-0.3$ and let $P=0$ to evaluate db/dP . In Fig. 4(a), the upper solid line is drawn according to Eq. (3). At this time, the pressure coefficients of the band gap become smaller than that obtained from linear interpolation. Even in this way, the pressure coefficients of PL peaks are still much lower than those of the corresponding band gaps except for sample B. For sample B ($x=0.08$), the pressure coefficient of the PL peak is lower than that of the band gap evaluated by linear interpolation, while it is very near to that of the band gap calculated by Eq. (3). For thin-film samples, on the other hand, the difference of the compressibility between epilayer and substrate may add biaxial strains to the heterostructure. The strains will induce a decrease of the pressure coefficient of the epilayer.¹⁹ According to Rockwell's model,²⁰ we evaluated the pressure-induced strains in the ZnSTe/GaAs structure for the pseudomorphic situation. The decrease of pressure coefficients due to that effect is less than 2%. Considering that the thickness of the epilayer of our samples is about 1 μm , the effect of strains on the pressure coefficients will be insignificant.

It is well known that the smaller pressure coefficient of the PL peak than that of the corresponding band gap is a typical characteristic of deep levels. All the arguments above support that the emission peaks in our experiment reasonably originate from the radiative recombination of excitons trapped at Te_n ($n \geq 2$) isoelectronic centers. Because the trapping potentials of Te_n ($n \geq 2$) isoelectronic centers are rather localized, the wave functions of hole trapped on them should be a mixture of the wave functions of the whole valence bands and which leads to the great difference of the pressure behaviors between the PL spectra of isoelectronic centers and corresponding band gap in $\text{ZnS}_{1-x}\text{Te}_x$ alloys.

Sample B ($x=0.08$) has a large binding energy and larger pressure coefficient. In Fig. 4(b) we draw the variation of the difference of the pressure coefficient of the band gap and the PL peak energy, $dE_b/dP = dE_g/dP - dE_{PL}/dP$, as a function of relative binding energy, $\varepsilon_b = (E_g - E_{PL})/E_g$. The Te composition x is labeled near the data point. We can see that the pressure coefficient of the binding energy dE_b/dP increases monotonically with a decrease in ε_b . This

shows that the pressure behaviors of Te_n isoelectronic centers are tightly related to the depth of these levels apart from the top of the valence band.

Beyond our expectation, it is found in Fig. 4(b) that the pressure coefficient of the binding energy dE_b/dP increases when ε_b becomes smaller. If the PL spectra come from larger Te_n clusters when the Te composition value x is higher, the range of the localized potential of larger clusters should be more extended. This will result in similar pressure behavior of Te_n centers to that of the band gap. Even if all the PL spectra come from the same Te_n clusters, the smaller difference between the localized potential of Te_n clusters and host potential of $\text{ZnS}_{1-x}\text{Te}_x$ should also lead to a smaller difference of the pressure coefficient of the Te_n clusters and band gap.

According to the calculation of Hennig and co-workers using the Koster-Slater model in the one-band one-site approximation,^{14,15} the binding energy E_b for the bonding state of Te_2 clusters can be expressed as

$$E_{b,bond} = \frac{1}{2} \left[J - \frac{3}{2}T + \left(J + \frac{T}{2} \right) \sqrt{1 + \frac{T}{2J}} \right], \quad (7)$$

in which J is the matrix element of the Te_2 isoelectronic potential in Wannier representation and T is the bandwidth of the valence band in a semielliptic Hubbard density approximation.²¹ It should be noticed that the binding energy in Eq. (7) is defined as the difference between the zero-phonon line of bound excitons and the emission band of free excitons. Here, we neglect its difference with our definition of the binding energy. For other Te_n ($n=1,3$, and 4) isoelectronic centers the binding energy E_b is also related to J and T .¹⁵ We can see that the pressure coefficient of the binding energy E_b is related to both dJ/dP and dT/dP . The smaller binding energy reflects a smaller localized potential. It may then result in a smaller dJ/dP . On the other hand, dT/dP for different $\text{ZnS}_{1-x}\text{Te}_x$ alloys with different Te compositions x should be distinct, because the pressure coefficients of ZnS and ZnTe are very different. The Te composition dependence of dE_b/dP is then determined by these two effects. The change in dT/dP with Te composition may be the main reason for the abnormal increase of dE_b/dP when ε_b decreases. However, more theoretical analysis is expected to testify to our assumption.

C. Pressure dependence of PL intensities

We also investigated the integrated intensity of PL spectra as a function of pressure. Figure 5 shows the pressure dependences of the integrated intensities of samples A ($x=0.02$) and C ($x=0.15$). With the increase of pressure, the integrated intensities decrease nonlinearly. Similar results are obtained from other samples. In Ref. 6, we have measured the pressure dependence of the integrated PL intensities of sample D ($x=0.21$) excited by 406.7 nm and 488.0 nm lines, respectively. And we have proved that the decrease of the integrated intensity of PL spectra is due to the descent of the absorption efficiency from deep centers to the conduction band. This descent results from the approach of the distance

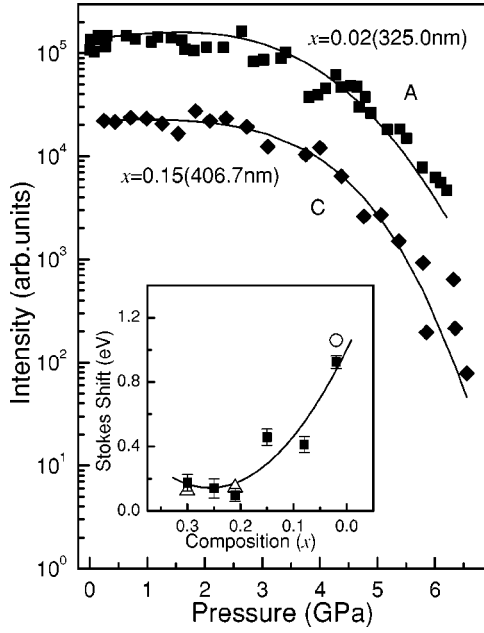


FIG. 5. The pressure dependences of the integrated intensities of sample A (solid squares) and C (solid diamonds). Solid lines are fitting result by Eq. (8). The variation of the Stokes shift E_S (solid squares) as a function of x is shown in the inset together with the PLE result (open circle) and the activation energies (open triangles).

between the deep centers and conduction band to the laser energy. According to the research of Te isoelectronic centers in ZnS, there exists a large Stokes shift E_S between its emission band and the absorption band because of the lattice relaxation.^{7,10} If we describe the density of states of the Te_n isoelectronic centers by a Gaussian function with half-width G and assume that E_S and G are independent of pressure, we can express the integrated intensity of the PL peak under pressure as⁶

$$I = C \int \frac{(E_i + \hbar\omega - E_{C0})^{3/2}}{(E_i - E_{V0})^{3/2} \left(1 + \frac{E_i + \hbar\omega - E_{C0}}{E_i - E_{V0}}\right)^4} \times \exp\left(-\frac{(E_i - E_{i0})^2}{(G/2)^2}\right) dE_i, \quad (8)$$

where E_{V0} and E_{C0} are the energy of the top of the valence band and the bottom of the conduction band, respectively; E_{i0} is the central position of the absorption band; $\hbar\omega$ is the photoenergy; and C is a constant. According to the model above, the central position of the absorption band E_{i0} under hydrostatic pressure is expressed by

$$E_{C0} - E_{i0} = E_{PL}(P) + E_S = E_{PL}(0) + \alpha P + E_S. \quad (9)$$

If we take the top of the valence band as zero, then $E_{V0} = 0$ and

$$E_{C0} = E_g = E_g(0) + \alpha' P, \quad (10)$$

where $E_g(0)$ is the band gap under normal pressure and α' is the pressure coefficient of the band gap. With taking the

Stokes shift E_S , half-width of the absorption band G , and constant C as fitting parameters, we fitted the measured integrated intensities of each sample by Eqs. (8), (9), and (10). The fitting results of sample A ($x=0.02$) and C ($x=0.15$) are shown in Fig. 5 with solid lines. The values of E_S for each sample are listed in Table I. Since the PL peak was near to the laser energy (406.7 nm) for sample A in Ref. 6, we remeasured the data of sample A by using a 325.0 nm laser line. Because the laser energy of 325.0 nm is higher than the band gap of sample A in the pressure range of 0–3.5 GPa, the absorption from valence band to conduction band should be considered. However, it will induce more fitting parameters and make the fitting procedure more complicated. Therefore we did not include the band-to-band absorption in our fitting. We obtained the Stokes shift E_S of sample A as 920 meV, which is near to the Stokes shift of Te_2 isoelectronic centers, 930 meV, reported by Fukushima and Shionoya.⁷ The fitting result is also in good agreement with our PL excitation (PLE) experiment that gives a Stokes shift of about 1.0 eV from sample A. In the inset figure of Fig. 5, we draw the variation of the Stokes shift E_S (solid squares) as a function of Te composition x . The solid line is just a guide for the eye. For comparison, the value of E_S (open circle) measured by PLE spectra for sample A and the activation energies (open triangles) measured by the temperature dependence PL spectra for sample D ($x=0.21$) and F ($x=0.30$) (Ref. 11) are depicted too. Although the activation energy is different with the Stokes shift, they have the same magnitude. Thus these data from experiment further testify that the Stokes shifts fitted from our model above are reliable. We can see that the Stokes shift E_S decreases with increasing Te composition. As discussed above, the PL spectrum of sample A ($x=0.02$) comes from Te_2 isoelectronic centers and that of sample B ($x=0.08$) or other samples with larger x from Te_3 or larger Te_n clusters. Goede *et al.*¹³ have shown that the larger Te_n clusters have smaller lattice relaxation in CdTe alloys. The decrease of the difference between potentials of the localized clusters and host atoms will lead to a descent of lattice relaxation. Then, the decrease of E_S with an increase of x is a reasonable result.

IV. SUMMARY AND CONCLUSION

The PL emission bands of $\text{ZnS}_{1-x}\text{Te}_x$ ($0.02 \leq x \leq 0.3$) alloys with six different Te compositions values have been measured under hydrostatic pressure at room temperature. These emission bands originate from the excitons trapped at Te_n ($n \geq 2$) isoelectronic centers, $n=2$ for the sample with $x=0.02$, and $n \geq 3$ for samples with higher composition values. The pressure coefficients of the emission bands are smaller than those of the corresponding band gaps of alloys. It is a characteristic of the deep levels. The variation of the pressure coefficient as a function of Te composition is discussed. It seems tightly related to the binding energy of Te_n centers. The pressure coefficient of the binding energy of Te_n centers increases with a decrease of the relative binding energy. This phenomenon needs further theoretical analysis.

The decrease of integrated intensities with pressure is attributed to the decrease of absorption efficiency when the absorption band approaches the laser line under higher pressure. The Stokes shift of Te_n centers is then calculated from this model. The decrease of the Stokes shift with increasing Te composition is in agreement with our expectation.

ACKNOWLEDGMENTS

This work was partly supported by the National Natural Science Foundation of China under Contact No. 60176008 and the Hong Kong Research Grant Council (RGC) (HKUST6125/98P).

-
- ¹D.J. Wolford, J.A. Bradley, K. Fry, and J. Thompson, in *Proceedings of the 17th International Conference on the Physics of Semiconductors*, edited by J.D. Chadi and W.A. Harrison (Springer-Verlag, New York, 1984), p. 627.
- ²W. Shan, W. Walukiewicz, J.W. Ager III, E.E. Haller, J.F. Geisz, D.J. Friedman, J.M. Olson, and S.R. Kurtz, *Phys. Rev. Lett.* **82**, 1221 (1999).
- ³W. Walukiewicz, W. Shan, K.M. Yu, J.W. Ager III, E.E. Haller, I. Miotkowski, M.J. Seong, H. Alawadhi, and A.K. Ramdas, *Phys. Rev. Lett.* **85**, 1552 (2000).
- ⁴W.K. Ge, S.B. Lam, I.K. Sou, J. Wang, Y. Wang, G.H. Li, H.X. Han, and Z.P. Wang, *Phys. Rev. B* **55**, 10 035 (1997).
- ⁵I.K. Sou, K.S. Wong, Z.Y. Yang, H. Wang, and G.K.L. Wong, *Appl. Phys. Lett.* **66**, 1915 (1995).
- ⁶N.Z. Liu, G.H. Li, W. Zhang, Z.M. Zhu, H.X. Han, Z.P. Wang, W.K. Ge, and I.K. Sou, *Phys. Status Solidi B* **211**, 163 (1999).
- ⁷T. Fukushima and S. Shionoya, *Jpn. J. Appl. Phys., Part 1* **12**, 549 (1973).
- ⁸A. Abdel-Kader, F.J. Bryant, and J.H.C. Hong, *Phys. Status Solidi A* **81**, 333 (1984).
- ⁹O. Goede, W. Heimbrod, T. Lau, G. Matzkeit, and B. Selle, *Phys. Status Solidi A* **94**, 259 (1986).
- ¹⁰W. Heimbrod and O. Goede, *Phys. Status Solidi B* **135**, 795 (1986).
- ¹¹N.Z. Liu, G.H. Li, Z.M. Zhu, H.X. Han, Z.P. Wang, W.K. Ge, and I.K. Sou, *J. Phys.: Condens. Matter* **10**, 4119 (1998).
- ¹²A. Reznitsky, S. Permogorov, S. Verbin, A. Naumov, Yu. Korostelin, V. Novozhilov, and S. Prokov'ev, *Solid State Commun.* **52**, 13 (1984).
- ¹³O. Goede, W. Heimbrod, and R. Müller, *Phys. Status Solidi B* **105**, 543 (1981).
- ¹⁴D. Hennig, O. Goede, and W. Heimbrod, *Phys. Status Solidi B* **113**, K163 (1982).
- ¹⁵O. Goede and D. Hennig, *Phys. Status Solidi B* **119**, 261 (1983).
- ¹⁶K. Strossner, C. Ves, C. K. Kim, and M. Cardona, *Solid State Commun.* **61**, 275 (1987); S. Ves, V. Schwarz, N. E. Christensen, K. Syassen, and M. Cardona, *Phys. Rev. B* **42**, 9113 (1990).
- ¹⁷R. Hill and D. Richardson, *J. Phys. C* **6**, L115 (1973).
- ¹⁸F.D. Murnaghan, *Proc. Natl. Acad. Sci. U.S.A.* **30**, 244 (1944).
- ¹⁹J.A. Tuchman and I.P. Herman, *Phys. Rev. B* **45**, 11 929 (1992).
- ²⁰B. Rockwell, H.R. Chandrasekhar, M. Chandrasekhar, A.K. Ramdas, M. Kobayashi, and R.L. Gunshor, *Phys. Rev. B* **44**, 11 307 (1991).
- ²¹J. Hubbard, *Proc. R. Soc. London, Ser. A* **A276**, 238 (1963).